Satellite estimation of photosynthetically active radiation in Southeast Asia: Impacts of smoke and cloud cover

Hideki Kobayashi,[1] Tsuneo Matsunaga,[2] Akira Hoyano,[1] Masatoshi Aoki,[3] Daisuke Komori,[4] and Samakkee Boonyawat[5]

Received 26 May 2003; revised 12 December 2003; accepted 17 December 2003; published 21 February 2004.

[1] Since large-scale variations in photosynthetically active radiation (PAR) influence the terrestrial carbon sources and sinks through the plant photosynthesis variations, large-scale evaluation of PAR is required. In the present study a simple PAR estimation model was developed for Southeast Asia, where large-scale forest fires occurred during El Niño years. The model considered the smoke aerosol released by forest fires using satellite-based smoke detection methods. A comparison study with ground-based solar radiation data for Malaysia and Thailand indicated that the current model could estimate monthly PAR with 10% (root-mean-square) accuracy and would successfully trace the seasonal and year-to-year variations in PAR, including the forest fire periods. During the peak-smoke month in Indonesia, September 1997, the reduction of PAR by smoke reached 63–75% in the center of the Kalimantan and Sumatra Islands. From the analyses of the smoke and cloud cover impacts on PAR in 1997–1999, annual PAR variations were found to be mostly regulated by smoke variations on the Malay Peninsula, Sumatra, and Kalimantan Islands and cloud cover variations on the Indo-China Peninsula. Thus annual variations in PAR changed with location. These variations did not simply correlate with year-to-year variations in cloud cover associated with the El Niño and La Niña cycle, but exhibited more complicated spatial variations due to the existence of smoke in Southeast Asia. *INDEX TERMS:* 0315 Atmospheric Composition and Structure: Biosphere/atmosphere interactions; 1640 Global Change: Remote sensing; 1615 Global Change: Biogeochemical processes (4805); *KEYWORDS:* photosynthetically active radiation, smoke, net primary production

Citation: Kobayashi, H., T. Matsunaga, A. Hoyano, M. Aoki, D. Komori, and S. Boonyawat (2004), Satellite estimation of photosynthetically active radiation in Southeast Asia: Impacts of smoke and cloud cover, *J. Geophys. Res.*, *109*, D04102, doi:10.1029/2003JD003807.

1. Introduction

[2] Estimates of regional carbon budgets are of particular interest in the tropics where much uncertainty regarding carbon sources and sinks still remains [*Gurney et al.*, 2002]. Recent studies suggest that the reduction in total photosynthetically active radiation (PAR) and the changes in the ratio of diffuse PAR significantly influence the terrestrial plant photosynthesis [*Chameides et al.*, 1999; *Cohan et al.*, 2002; *Gu et al.*, 2002, 2003; *Nemani et al.*, 2003; *Reichenau and Esser*, 2003]. For example, *Gu et al.* [2002, 2003] discussed the contribution of the diffuse PAR for the net primary production and showed that the increase in diffuse PAR caused by Mount Pinatubo's volcanic aerosol enhanced plant photosynthesis in a deciduous forest in North America. *Nemani et al.* [2003] suggested that increasing trend in PAR due to the reduction of cloud cover enhanced net primary production (NPP) in Amazon, while they did not consider the issues of diffuse PAR by cloud cover changes. As revealed in these studies, PAR variation significantly affects the NPP variation, and therefore reliable estimation of large-scale PAR is required for evaluating carbon fixation by plant photosynthesis.

[3] In Southeast Asia, large-scale forest fires occurred in 1997 and 1998 and emitted much smoke into the atmosphere [*Page et al.*, 2002]. These events had a great impact on the local environment and led to a reduction of plant photosynthesis through a reduction in PAR at the surface [*Davies and Unam*, 1999; *Toma et al.*, 2000; *Mori*, 2000; *Ishida et al.*, 2000]. Furthermore, interannual climate variations during the El Niño (1997–1998) and La Niña (1998–1999) periods changed the fraction of cloud cover. These weather phenomena may result in the temporal PAR variation and, consequently, NPP variation. *Tang et al.* [1996] investigated the light reduction due to smoke and its effect on leaf photosynthesis by ground-based and simulation studies in Malaysia. The Tang et al. study

[1]Interdisciplinary Graduate School of Science and Engineering, Tokyo Institute of Technology, Yokohama, Kanagawa, Japan.
[2]Social and Environmental Systems Division, National Institute for Environmental Studies, Tsukuba, Ibaraki, Japan.
[3]Faculty of Agriculture, Tokyo University of Agriculture and Technology, Tokyo, Japan.
[4]United Graduate School of Agricultural Science, Tokyo University of Agriculture and Technology, Tokyo, Japan.
[5]Faculty of Forestry, Kasetsart University, Bangkok, Thailand.

0148-0227/04/2003JD003807

concluded that the heavy smoke significantly affected photosynthesis, especially in the understory plants. As implied in these studies, PAR regulation of NPP may play an important role in Southeast Asia; however, previous studies had not evaluated the impact of large-scale PAR variation on NPP because of a lack of reliable spatial information on PAR.

[4] In previous studies, several PAR estimation models for global and continental scales have been developed for NPP estimation [*Frouin et al.*, 1989; *Frouin and Pinker*, 1995; *Eck and Dye*, 1991; *Pinker and Laszlo*, 1992; *Gu and Smith*, 1997]. Reanalysis radiation data sets are also often used for NPP estimation [*Running et al.*, 1999]. However most of these models and reanalysis data sets do not consider the impact of smoke on PAR in their model formulations. Although *Gu and Smith* [1997] partially discussed this issue in the Boreal Ecosystem-Atmosphere Study (BOREAS) using surface visibility data, they did not evaluate spatial variations in PAR in the smoke-affected areas.

[5] A lack of quantitative analysis data for spatial and temporal variations in smoke aerosol has prevented estimates of PAR in smoke-affected areas. Recently, several researchers proposed satellite-based smoke detection methods. *Herman et al.* [1997] developed the aerosol index (AI) based on the spectral contrast between two UV-A channels of a Total Ozone Mapping Spectrometer (TOMS) for UV-absorbing aerosol detection such as smoke. *Torres et al.* [1998, 2002] developed the aerosol optical thickness (AOT) estimation method through an inversion of the radiative transfer model using TOMS UV-A data. The aerosol information retrieved by these methods makes it possible to provide realistic PAR variation estimates for Southeast Asia.

[6] In the present study we focused on the total PAR (direct and diffuse PAR) over land. First, we developed a satellite-based PAR estimation method to evaluate the smoke-affected areas as well as the areas without smoke. Then, we estimated the monthly mean PAR in Southeast Asia (20°N–10°S, 90°E–130°E; Figure 1) from 1997 to 1999 and compared the estimates with ground-based total solar radiation and National Center for Environmental Prediction/National Center for Atmospheric Research (NCEP/NCAR) reanalysis data [*Kalnay et al.*, 1996]. Finally, we discussed the spatial and temporal variations in PAR and the impacts of smoke and cloud cover changes.

2. PAR Estimation Model

[7] The PAR estimation model is required (1) to be simple enough to reduce computational time and (2) to consider the PAR reduction caused by smoke. To meet these requirements, we developed the daily total surface incident PAR (MJ m^{-2} d^{-1}; hereinafter we simply use PAR.) estimation model using satellite data.

2.1. Model Description

[8] PAR can be calculated as a product of atmospheric transmittance and extraterrestrial solar radiation in 400–700 nm:

$$\mathrm{PAR} = \mathrm{PAR}_{\mathrm{TOA}} T_g T_{ra} T_c \tag{1}$$

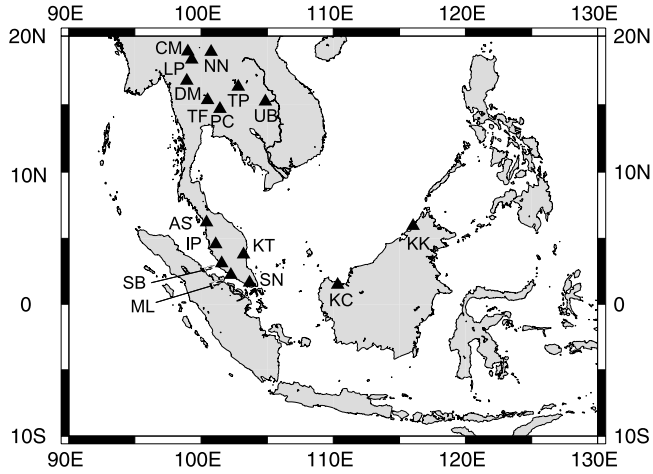

Figure 1. The study area. Triangles show the ground-based global solar radiation observation sites. (KK, Kota Kinabalu, 5.9°N, 116.05°E; KC, Kuching, 1.48°N, 110.33°E; ML, Malacca, 2.22°N, 102.25°E; SN, Senai, 1.63°E, 103.67°E; SB, Subang, 3.12°N, 101.55°E; KT, Kuantan, 3.78°N, 103.22°E; IP, Ipoh, 4.57°N, 101.10°E; AS, Alor Setar, 6.20°N, 100.40°E; PC, Pakchong, 14.70°N, 101.42°E; UB, Ubonrachatani, 15.25°N, 104.87°E; TF, Tak Fa, 15.35°N, 100.50°E; TP, Tha Prha; DM, Doi Musoe, 16.33°N, 102.82°E; LP, Lampang, 18.30°N, 99.30°E; NN, Nan, 18.87°N, 100.75°E; and CM, Chaing Mai, 18.90°N, 99.01°E).

where $\mathrm{PAR}_{\mathrm{TOA}}$ is the daily total PAR at the top of the atmosphere and T_g, T_{ra}, and T_c are atmospheric transmittances: T_g for gas absorption, T_{ra} for the Rayleigh scattering, aerosol scattering, and absorption, and T_c for cloud scattering. For the transmittance terms, we treated direct and diffused sky components together.

[9] Since gas absorption in the PAR spectral region is mainly caused by ozone, we considered only ozone absorption. *Frouin et al.* [1989] estimated T_g in the broad spectral interval using the exponential function of the ozone amount for instantaneous PAR estimation over oceans. We estimated T_g by slightly modifying their equation to consider the air mass at arbitrary elevations:

$$T_g = \exp\left\{-a_o (U_o m^*)^{bo}\right\} \tag{2}$$

where a_o and b_o are model coefficients determined by *Frouin et al.* [1989]. U_o and m^* are the total column ozone amount (atm-cm) and the effective air mass for daily basis estimation. We assumed $U_o = 0.25$ as a constant in our analysis because PAR sensitivity to the changes of the ozone amount is smaller than other parameters. The m^* can be calculated as a function of pressure (p) at the ground level

$$m^* = (p/p_0)m \tag{3}$$

where p/p_0 is the elevation correction factor for the effective air mass (m). We set p_0 (pressure at 0 m) to be 1013.25 (hPa) and used the hydrostatic equilibrium equation and GTOPO30 (approximately 1 km resolution) elevation data for

Table 1. Aerosol Type Dependent Model Coefficients Determined by Regression Analysis Using 6S

	Smoke	Continental
a	0.0287	0.0390
b	0.331	0.217
c	1.99	0.0100

p calculation. The m was estimated from air mass at noon (m_n) using the *Goldberg and Klein* [1980] equation:

$$m = \alpha_0 + \alpha_1 m_n + \alpha_2 m_n^2 \quad (m_n = 1/\cos(\theta_{noon})) \tag{4}$$

where α_0, α_1, and α_2 are coefficients determined by *Goldberg and Klein* [1980] and θ_{noon} is a solar zenith angle at noon.

[10] The attenuation due to Rayleigh scattering and aerosol scattering/absorption largely depends on the AOT. In exact PAR calculations, we need to take into consideration the spectral dependency of AOT in the PAR spectral region. However, we parameterized T_{ra} as a function of monochromatic value of AOT at 550 nm (τ_{550}) and θ_{noon} for model simplicity. When PAR is exponentially reduced in the atmosphere and multiple interactions between atmosphere-surface systems are considered, T_{ra} is calculated by

$$\begin{aligned} T_{ra} &= \exp\{-(a+b\tau_{550})m^*\}\left(1 + R_s S + (R_s S)^2 + (R_s S)^3 + \ldots\right) \\ &= \exp\{-(a+b\tau_{550})m^*\}/(1 - R_s S) \quad (S = c\ln(\tau_{550}+1)) \end{aligned} \tag{5}$$

where R_s is the mean surface reflectance in the PAR spectral region and a, b, and c are aerosol type dependent coefficients. S is the reflectance of the aerosol layer for the radiation backscattered to the surface. S was expressed as a logarithm function of τ_{550}. We assumed R_s to be 0.1.

[11] The a, b, and c were determined by regression analyses using the calculated PAR by the 6S radiative transfer model [*Vermote et al.*, 1997] under cloud-free conditions as summarized in Table 1. The regression analyses were carried out under various conditions for τ_{550} (0.06–0.7 for continental type, 0.4–6.8 for smoke type) and θ_{noon} (0–45 degree) under the tropical atmospheric profile. Single scattering albedo (ω) of smoke particles assumed in the 6S radiative transfer model for the default biomass burning type is higher (ω = 0.97) than that observed in Singapore and Malaysia ($\omega \approx 0.90$ [*Nakajima et al.*, 1999; *von Hoyningen-Huene et al.*, 1999]). Therefore we modified ω in the PAR spectral region to be 0.90 in 6S calculation for smoke type aerosol.

[12] Figure 2 shows the comparison of the present PAR estimation model and 6S-based PAR calculation results with several aerosol and θ_{noon} conditions (0.06–0.7 for continental type, 0.4–6.8 for smoke type, θ_{noon} for 0, 22.5, 45 degree, cloud-free). The 6S-based daily PAR was calculated by integrating the instantaneous PAR with half-hour interval during the daytime. There were small but systematic differences depended on θ_{noon}. There are two reasons in these differences. We assumed that PAR was exponentially reduced in the atmosphere. Strictly speaking, however, PAR is not exponentially reduced due to radiation enhancement caused by the multiple interactions in the aerosol layer. This radiation enhancement depends on the θ_{noon} and AOT. Moreover, we used equation (4) for effective air mass on the daily basis estimation. The error of this function led to the differences in T_{ra}. The root-mean-square error (RMSE) in the present model was 0.22 MJ m^{-2} d^{-1} for continental aerosol condition and 0.14 MJ m^{-2} d^{-1} for smoke aerosol.

[13] The cloud transmittance (T_c) was calculated in a manner similar to *Eck and Dye* [1991] using the Lambert equivalent reflectivity (LER) derived from UV-A irradiance. *Krotkov et al.* [2001] investigated the theoretical background of the following equation for T_c calculation:

$$T_c = (1 - R_{sys})/(1 - R_{uvs}) = (1 - R_{uv})/(1 - R_{uvs}) \tag{6}$$

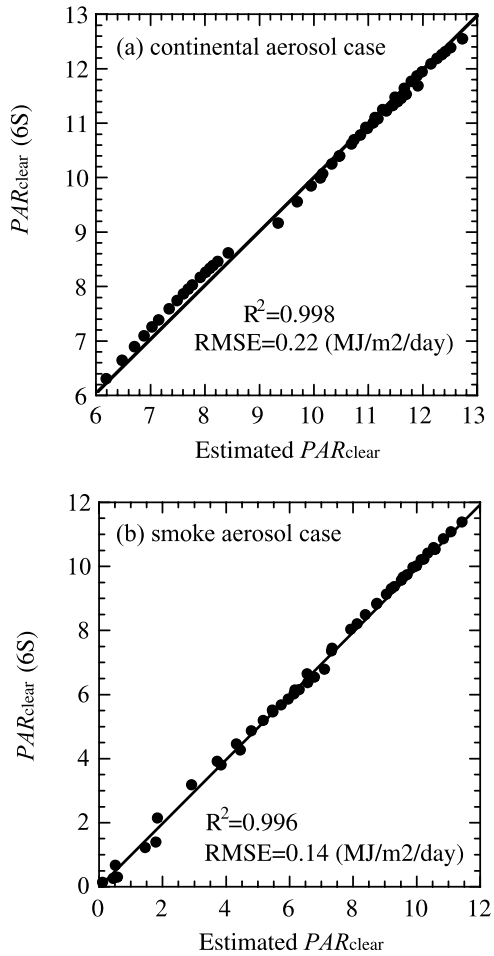

Figure 2. Comparison of PAR clear calculated by the present model and the 6S radiative transfer model. The comparison of the present model and 6S-based PAR calculation results was performed at various aerosol and θ_{noon} conditions (0.06–0.7 for continental type, 0.4–6.8 for smoke type, θ_{noon} for 0–45 degree, cloud-free condition). The 6S-based daily PAR was calculated by integrating the instantaneous PAR with half-hour interval during the daytime. (a) Continental aerosol case. (b) Smoke aerosol case.

where R_{sys}, R_{uv}, and R_{uvs} are a cloud-surface system reflectivity, a TOMS UV-A channel reflectivity (360 nm for Earth Probe/TOMS) [*McPeters et al.*,1998], and a surface reflectivity in UV-A spectral region. This is a generalized form of Eck and Dye's method for an arbitrary surface reflectivity. *Krotkov et al.* [2001] shows the equation (6) works well for snow-free conditions because the atmospheric effect on T_c is cancelled by the systematic lower trend of R_{uv} to R_{sys} owing to the TOMS observation geometry.

[14] Since spectral characteristics of cloud are similar in both UV-A and PAR spectral regions, Eck and Dye's method agreed well with surface pyranometer measurements [*Eck and Dye*, 1991; *Dye and Shibasaki*, 1995]. However, the backscattered radiation from smoke aerosol cannot be eliminated by equation (6). Therefore this effect must be corrected for T_c estimation.

[15] Smoke is generally emitted in the dry season with little cloud cover [*Hsu et al.*, 2003]. Moreover, it is close to surface in most cases since smoke is emitted from ground. From these considerations, we assumed that smoke-cloud interaction can be neglected and the aerosol layer is lower than the cloud layer. In these cases, cloud transmittance can be expressed as follows:

$$T_c = (1 - R_{uv})/(1 - R_{uvsa}) \tag{7}$$

where R_{uvsa} is a reflectance of the aerosol-surface system. Neglecting the higher-order scattering between aerosol and surface, R_{uvsa} is calculated by

$$R_{uvsa} = R_{uva} + T_{uvad}T_{uvau}R_{uvs} \tag{8}$$

The first term (R_{uva}) of equation (8) is the direct reflectance of the aerosol layer, and the second term ($T_{uvad}T_{uvau}R_{uvs}$) is the reflectance of the surface for the radiation through the aerosol layer, where T_{uvad} and T_{uvau} are transmittance of the aerosol layer for downward and upward irradiance. R_{uva} and $T_{uvad}T_{uvau}$ were calculated by the third-order polynomial regressions:

$$R_{uva} = -0.00285 + 0.0744x - 0.0107x^2 + 0.000532x^3 \quad \left(R^2 = 0.998\right) \tag{9}$$

$$T_{uvad}T_{uvau} = 0.998 - 0.454x + 0.0756x^2 - 0.00430x^3 \quad \left(R^2 = 0.996\right) \tag{10}$$

where x is $\tau_{360}/\cos(\theta)$. The coefficients of these regressions were determined by 6S model (τ_{360}, 0.0–5.0; θ, 0–50 degree).

[16] It should be noted that there is an exceptional case on the assumption in the equation (7) in northern Vietnam (above 18 degrees north). According to the detailed discussion by *Hsu et al.* [2003], smoke is often above the low-level thick cloud in the spring in this region. In this case, smoke-cloud interactions are complicated and cannot be represented by equation (7). Therefore we exclude this region in the following analysis.

2.2. AOT Estimation

[17] The PAR estimation model described in section 2.1 requires the spatial data sets of τ_{550} and τ_{360}. In the present section, we described the τ_{550} and τ_{360} estimation methods in both smoke-affected and nonsmoke areas.

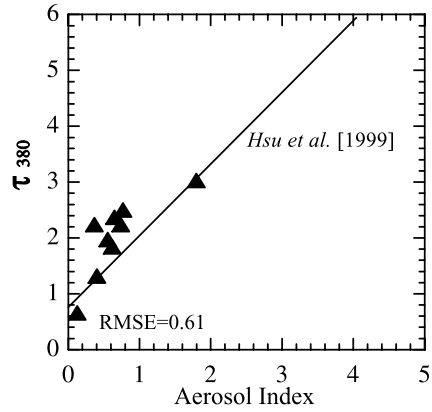

Figure 3. The relationship between τ_{380} and aerosol index (AI). Solid triangles indicate the relation between daily mean ground observed τ_{380} by *Nakajima et al.* [1999] and AI. The regression line obtained by *Hsu et al.* [1999] is also indicated in the figure.

2.2.1. AOT Estimation in Smoke-Affected Areas

[18] We used the AI for smoke detection. The AI has a large positive value (~5.0) in the presence of smoke. The AI is not directly related to AOT but is an index relevant to the amount of smoke aerosol. *Hsu et al.* [1999] found a linear relationship between AI and AOT (τ_{380}) with Sunphotometer measurements of African and South American smokes:

$$\tau_{380} = \beta_1 \mathrm{AI} + \beta_2 \tag{11}$$

The regression coefficients β_1, β_2 were depended on the single scattering albedo (ω) and smoke aerosol height. According to literatures, the ω in the presence of the smoke was about 0.9 in Singapore and Malaysia [*Nakajima et al.*, 1999; *von Hoyningen-Huene et al.*, 1999] and smoke aerosol height was 2–3 km [*von Hoyningen-Huene et al.*, 1999; *Koe et al.*, 2001]. Similar aerosol properties were observed in South America. *Schafer et al.* [2002] estimated ω between 0.89 and 0.91, and smoke height observed by *Andreae et al.* [1988] was between 1.5 and 3 km. Therefore we used β_1 = 1.25 and β_2 = 0.71 determined for South American type smoke by *Hsu et al.* [1999].

[19] To confirm the reliability of AI-AOT relationship predicted by equation (11), we compared AI and AOT (τ_{380}) relationship with the *Nakajima et al.*'s [1999] ground-based daily averaged data (Figure 3). In some cases, AOT prediction by equation (11) is lower than ground-based data; however, it is basically consistent with ground-based data.

[20] We estimated the AOT from the equation (11). The τ_{550} and τ_{360} were obtained from Angstrom's law. The Angstrom exponent was set at 1.0 referring to *Nakajima et al.* [1999].

2.2.2. AOT Estimation in Areas Without Smoke

[21] To estimate the τ_{500} and τ_{360} in nonsmoke areas, we used the ground-based daily mean surface visibility data. Daily visibilities were acquired from the Global Surface Summary of Day summarized by National Climatic Data Center (NCDC) of the National Oceanic and Atmospheric Administration (NOAA) [*NOAA*, 2002]. Daily visibilities

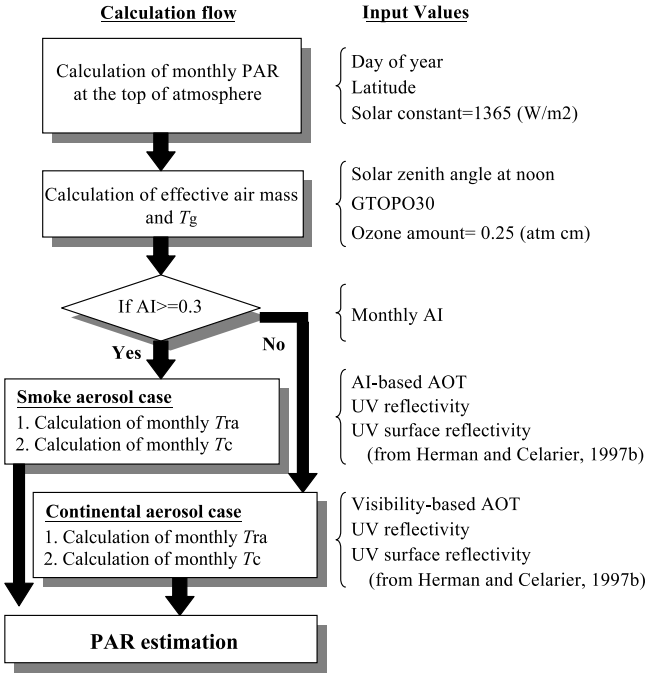

Figure 4. Satellite-based PAR estimation flow and input parameters. All calculation of this flow was performed for pixel-by-pixel in land pixels.

were averaged for each month at each station and converted to τ_{550} using the same formula adopted by 6S [*Vermote et al.*, 1997]:

$$\tau_{550} = 2.76V^{-0.8} \tag{12}$$

where V is visibility. Equation (12) is limited to $V > 5$ km because there are large uncertainties in low visibility. Generally, visibility was higher than 5 km, if there was no smoke and fog.

[22] The τ_{360} was obtained from Angstrom's law. The Angstrom exponent was set at 0.3, referring to *Nakajima et al.* [1999]. Calculated τ_{550} and τ_{360} in all stations were gridded by linear interpolation to obtain the spatial AOT distribution.

3. PAR Comparison With Ground-Based Data

3.1. Procedures of the PAR Estimation by Satellite Data

[23] Figure 4 shows the proposed PAR estimation flow. In the current study, we used EP/TOMS level-3 daily UV reflectivity and AI data [*McPeters et al.*, 1998]. The original spatial resolution of these data was 1.25 × 1.0-degree. Daily UV reflectivity and AI were averaged for a month and interpolated in 0.1 × 0.1 degree by the bilinear method. As UV surface reflectivity (R_{uvs}), we used *Herman and Celarier*'s [1997] annual mean R_{uvs} climatology data produced by minimum value composites of long-term Nimbus-7/TOMS UV reflectivity to screen out cloud reflection. R_{uvs} was also interpolated in 0.1 × 0.1 degree by the bilinear method.

[24] The monthly AI was used for pixel-by-pixel aerosol model selection. In the current PAR estimation flow, we regarded the AI > 0.3 as a smoke-affected area. AI = 0.3 is equivalent to the $\tau_{500} = 0.82$. On the other hand, τ_{500} of the background aerosol is less than 0.4 [*Nakajima et al.*, 1999]. Therefore, when AI is larger than 0.3, the smoke can be regarded as a principal component of the atmospheric aerosols. Moreover, the smoke detection by AI is limited down to 0.3 due to the low smoke sensitivity in AI < 0.3 [*Hsu et al.*, 1999]. When AI was greater than 0.3, T_{ra} and T_c were derived from smoke aerosol coefficients in Table 1 and AI-based AOT data. In other cases, T_{ra} and T_c were derived from continental aerosol coefficients and visibility-based AOT.

[25] The threshold of AI influences the smoke-affected area. In the current study, we used AI > 0.3 as a smoke detection criteria, and therefore small-scale smoke areas were not considered. Therefore the maximum differences between actual τ_{550} and estimated τ_{550} might become about 0.3 in small-scale smoke condition. This corresponds to 0.8 MJ m^{-2} d^{-1} differences at the maximum in PAR estimation. All calculations in the present study were carried out with 0.1-degree resolution.

3.2. Data Sets and Comparison Methods

[26] Comparisons between the estimated PAR and the ground-based data were conducted at the various sites located in Malaysia and Thailand to confirm the reliability of present PAR estimation results in Southeast Asia. In fact, there are few direct PAR ground observations in this region. Therefore we derived PAR from the ground-based total solar radiation data sets.

[27] Several researchers have revealed that the PAR ratio to total solar radiation (PAR_{ratio}) is around 0.48 [*Baker and Frouin*, 1987; *Pinker and Laszlo*, 1992; *Frouin and Pinker*, 1995;]. *Schafer et al.* [2002] investigated the PAR_{ratio} in smoke-affected and nonsmoke areas. They found daily mean PAR_{ratio} = 0.47 for the nonsmoke case but it fell to ~0.40 with the smoke increase ($\tau_{440} \approx 2.5$). On the basis of their results, we introduced the empirical formula to determine the most probable PAR_{ratio} when smoke detected (AI > 0.3).

$$PAR_{ratio} = 0.47 - 0.035\,\tau_{550} \tag{13}$$

The τ_{550} was calculated by equation (11) and Angstrom's law. In nonsmoke cases, we used 0.47 as a PAR_{ratio}. The uncertainties are around ±0.01 (=0.18 MJ m^{-2} d^{-1}) for nonsmoke cases and ±0.02 (=0.26 MJ m^{-2} d^{-1}) for smoke affected cases.

[28] As for the ground data in Malaysia, we used the monthly mean total solar radiation data from January 1997 to December 1999, observed by the Malaysian Meteorological Service. The locations of the eight observation sites in Malaysia are shown in Figure 1. In Thailand we observed total solar radiation from January 1998 to December 1999. The locations of the eight observation sites in Thailand are also shown in Figure 1. We only used monthly mean total solar radiation, whose number of the lack of measurements was less than three in a month. The number of available data for the comparison study was 457 of 480 data.

[29] Observed data from several sites were affected by heavy smoke, which was released in Indonesia and moun-

Table 2. Comparison of PAR Estimation Results and Ground-Based Pyranometer Data for Malaysia and Thailand[a]

		Site in Malaysia								
		KC	KK	AS	IP	SB	KT	ML	SN	Average
Average difference	This study	0.54	1.32	−0.94	0.08	0.25	0.25	−0.11	0.29	0.23
	NCEP/NCAR	2.31	2.48	0.77	1.04	1.09	1.59	0.66	1.91	1.60
RMSE	This study	0.65	1.39	1.04	0.41	0.42	0.49	0.42	0.52	0.60
	NCEP/NCAR	2.65	2.61	0.99	1.16	1.34	1.78	1.06	2.16	1.85
		Site in Thailand								
		DM	CM	TP	UB	LP	PC	NN	TF	Average
Average difference	This study	−0.16	−0.53	−0.20	−0.61	−0.21	−0.56	−0.15	−0.35	−0.36
	NCEP/NCAR	1.77	1.27	0.70	0.41	1.61	0.52	1.94	1.31	1.15
RMSE	This study	0.81	0.76	0.56	0.72	0.63	0.78	1.24	0.52	0.78
	NCEP/NCAR	1.62	2.04	1.49	0.92	2.28	1.05	2.62	1.83	1.58

[a]The average difference (MJ m^{-2} d^{-1}) indicates site-averaged difference between estimated PAR and ground data. RMSE (MJ m^{-2} d^{-1}) is a root-mean-square error.

tainous regions in Thailand; therefore it is possible to evaluate the validity of smoke aerosol parameterization in our model. In addition, downward short wave radiation data, derived from the NCEP/NCAR reanalysis, and PAR estimation results calculated by *Eck and Dye*'s [1991] model were used to compare the characteristics of their data and the present estimation results. These data are often used in NPP estimation studies. The original spatial resolution of NCEP/NCAR data was about 1.88 × 1.91-degree. Daily NCEP/NCAR data was averaged for a month and interpolated in 0.1 × 0.1-degree by the bilinear method. We converted the NCEP/NCAR downward short wave radiation to PAR by multiplying by 0.47.

3.3. Results of Monthly PAR Comparison

[30] Table 2 shows the average difference (AD) between estimated PAR and ground data as well as the root-mean-square errors (RMSE) at all sites. Positive ADs indicate that the estimation tends to be larger than the ground data.

[31] The results suggest that RMSEs in the present model were 0.6 MJ m^{-2} d^{-1} in Malaysia and 0.78 MJ m^{-2} d^{-1} in Thailand. The results also suggest that ADs in the present model have a different tendency in each country. It was positive at almost all sites in Malaysia and negative at all sites in Thailand. The main reason is the accuracy of AOT estimation. As described in section 2.2.2, the AOT in nonsmoke areas was estimated from surface visibilities and country-dependent variation was found in the visibility-based AOT. Average τ_{550} was 0.31 ± 0.08 in Malaysia and 0.45 ± 0.09 in Thailand. This difference is equivalent to the 0.5 MJ m^{-2} d^{-1} for PAR estimation. Also, some errors in the present model might be attributed to the cloud and smoke variations within daily or monthly timescales [*Gu et al.*, 2001] because the influence of these short timescales was neglected in the present model. In the NCEP/NCAR case, PAR did not have a different tendency between two countries; however, PAR was largely overestimated for all sites.

[32] Table 3 shows the year-to-year change of AD and RMSE. The estimation accuracy varies with the year. The AD and RMS are approximately 2–6% and 10%, respectively. Figure 5 shows the seasonal variation of PAR in Kuching (KC) and Chiang Mai (CM). There were the heavy smoke impacts from August to November 1997 and from March to April 1998 in KC because of its location on the lee side of the Indonesian forest fires [*Davies and Unam*, 1999]. The results of the present model show seasonal variations similar to the ground data, including during the heavy smoke periods. Results in CM also show similar seasonal variations including during the forest fire period in March 1998.

[33] In contrast, NCEP/NCAR data show weak seasonal variations during the periods without smoke and large overestimation during all smoke-affected periods. As mentioned by *Kalnay et al.* [1996], no actual observation inputs associated with cloud cover and smoke aerosol are used for downward short wave radiation calculations. Thus the downward short wave radiation is derived solely from the climate model in the NCEP/NCAR. As a result, this leads to a deterioration of the NCEP/NCAR data quality. NCEP/NCAR reanalysis is useful because it provides globally uniform data in the long term; however, it is difficult to use these data for seasonal and multiyear analyses of NPP in the tropics.

[34] Figure 5 also shows that *Eck and Dye*'s [1991] model has large overestimations during all smoke-affected periods due to the lack of smoke aerosol parameterization. In nonsmoke seasons, their model results were usually higher than ground data, because it assumes thin aerosol in their atmospheric turbidity factor.

[35] Thus the seasonality of PAR predicted by the present model agreed well with that of ground measurements in Malaysia and Thailand including the smoke-affected periods (RMS 10%). Since we neglected the smoke-cloud interactions and assumed that the smoke was lower than cloud in our model formulation, the model will be limited to

Table 3. Comparison of PAR Estimation Results and Ground-Based Pyranometer Data[a]

	Average Difference, MJ m^{-2} d^{-1}	RMSE, MJ m^{-2} d^{-1}
	Malaysia	
1997	0.21 (2.7%)	0.75 (9.6%)
1998	0.16 (2.0%)	0.76 (9.3%)
1999	0.30 (3.8%)	0.74 (9.2%)
	Thailand	
1998	−0.46 (5.9%)	0.75 (9.5%)
1999	−0.26 (3.5%)	0.81 (10.9%)

[a]Root-mean-square error and average difference were calculated using data from all sites in Malaysia and Thailand.

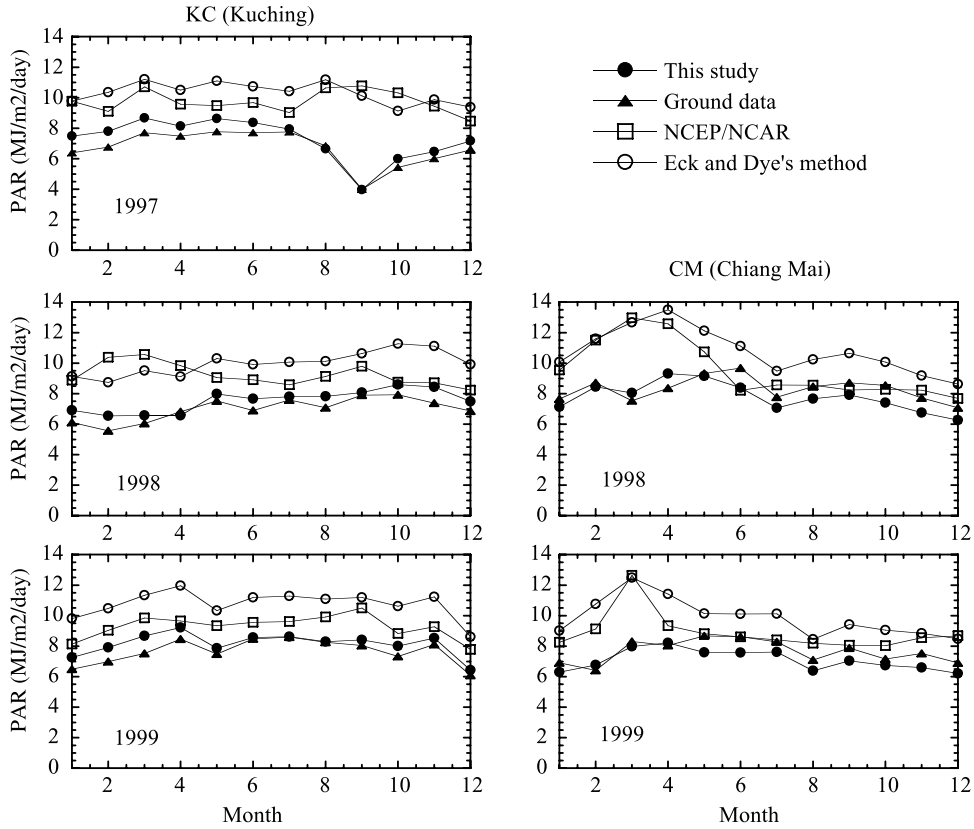

Figure 5. Seasonal and interannual PAR variations in Kuching (1.483°N, 110.33°E) and Chaing Mai (18.9°N, 99.01°E).

these conditions. The large-scale smoke in the tropics occurs mostly in the dry season. It indicates that the assumptions in the current model are reasonable in the most smoke-affected regions. However, it may be impossible to detect the small-scale smoke from local fires due to the coarse spatial resolution of the TOMS AI. Moreover, small-scale smokes can occur even in wet seasons with many clouds. In this case, smoke-cloud interactions cannot be neglected.

[36] Also, we focused mainly on the smoke-dominated case. In the smoke, dust, and sulfur dioxide mixed regions such as China [*Chu et al.*, 2003] and Japan [*Aoki and Fujiyoshi*, 2003], it should be needed to establish the alternative AI and AOT relationships or to use aerosol information derived from other satellite sensors such as MODIS.

3.4. Effect of Day-to-Day PAR Variations on Monthly Mean PAR

[37] In the previous section we discussed monthly based comparisons. However, the smoke that occurred in Thailand has large day-to-day variations. To evaluate the effect of day-to-day PAR variations on monthly averaging PAR, we estimate the daily PAR using daily UV reflectivity and AI data in a smoke dominated month, March, in Chiang Mai, Thailand. In this site, PAR has large day-to-day variations associated with day-to-day smoke variations, so we can see how day-to-day PAR variations affect the monthly PAR.

[38] Figure 6 shows the day-to-day variations in estimated PAR and ground-based data. The estimated PAR was fairly

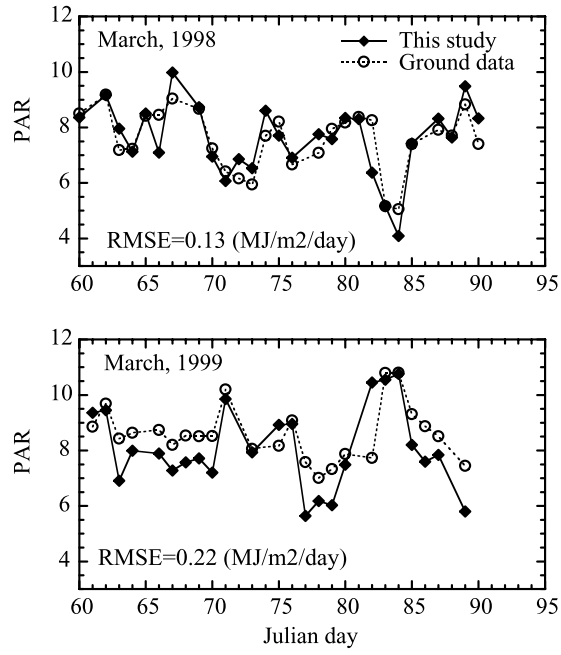

Figure 6. Day-to-day variations in PAR induced by smoke variations in March 1998 and 1999 in Chaing Mai, Thailand. Diamonds indicate this study; circles indicate ground data.

Table 4. The Effect of Monthly Basis PAR Averaging on Day-to-Day PAR Variations Induced by Smoke Variations in Chiang Mai, Thailand, in March[a]

	Ground Data	PAR From Monthly Data	PAR From Daily Data
1998	7.54	8.05	7.61
1999	8.31	7.98	8.07

[a]Units are MJ m^{-2} d^{-1}. Monthly based PAR was calculated using monthly based aerosol and cloud data, and daily based PAR was firstly calculated using daily data, and then monthly averaged.

consistent with ground-based data. RMSEs in daily based estimations are 0.13 MJ m^{-2} d^{-1} in 1998 and 0.22 MJ m^{-2} d^{-1} in 1999. Table 4 summarizes the estimated PAR results using monthly aerosol/cloud values and using daily values. The daily estimation was more accurate in both 1998 and 1999. These differences were less than 6%, and the effect of day-to-day PAR variations on monthly averaging PAR was considered to be about 6% at the maximum.

4. Smoke and Cloud Cover Impacts on PAR Variations

4.1. Smoke Impacts During the Indonesian Forest Fire Period

[39] In Indonesia, two large forest fire events were recorded between 1997 and 1998. During the 1997 event (August to November 1997), forest fires mainly occurred in Central Kalimantan and the Sumatra Islands and peaked in September 1997 [*Wooster and Strub*, 2002]. During the 1998 event (January to April 1998), forest fires mainly occurred in East Kalimantan [*Mori*, 2000] and peaked in March 1998.

[40] Figure 7 shows PAR variations from September to December 1997. Large PAR reductions were found on Kalimantan Island, Sumatra Island, and the southern part of the Malay Peninsula due to smoke from forest fires on Kalimantan and Sumatra Islands. The PAR reduction by smoke lasted from August to November 1997. In September 1997, the month of peak smoke, PAR was only about 2–4 MJ m^{-2} d^{-1} in the center of Kalimantan and Sumatra. If the PAR is calculated using the typical AOT value (τ_{550} = 0.3), instead of the AOT obtained in the present study (τ_{550} = 2.5–4.5), the PAR reaches to 8–9 MJ m^{-2} d^{-1}. Thus the maximum PAR reduction by smoke reached 5–6 MJ m^{-2} d^{-1} (a 63–75% reduction).

[41] Figure 8 shows the area-averaged ratio of PAR in June 1997 to May 1998 to PAR in the corresponding month in 1999. The averaged area (10°N–6.6°S, 94.4°E–119°E) includes Kalimantan, Sumatra, and the southern part of the Malay Peninsula. There was no smoke impact in 1999, and it is therefore possible to evaluate the smoke impact on PAR. The PAR reduction coincided with the two forest fire events. The first forest fire event lasted temporally longer and spatially wider than the second one. In addition, wind directions in the summer season concentrated on the Malay Peninsula. Therefore the impact on PAR from the first forest fire was stronger than the impact from the second. Variations in the ratio of PAR range from 60 to 100%. Thus we found the extraordinary seasonal PAR variations to be affected by smoke. This should affect plant photosynthesis, as discussed by *Tang et al.* [1996].

4.2. Temporal Changes in PAR in Southeast Asia

[42] Large variations in the seasonal rainfall patterns were reported during the El Niño and La Niña years from ground observations [*Wooster and Strub*, 2002; *Toma et al.*, 2000]. Similarly, cloud cover may also have temporal variations. Variations in cloud cover and smoke result in the PAR variations. In this section we investigated the year-to-year variations in cloud cover and smoke and their impacts on PAR. As indicators of cloud cover and smoke, we used the cloud transmittance (T_c) in equation (7) and τ_{550} estimated in the present study.

[43] Figure 9 shows the area-averaged PAR, T_c, and τ_{550} variations. Figures 9a and 9b include the land in 10°N–6.6°S, 94.4°E–119°E (region A, Kalimantan, Sumatra, and the southern part of Malay Peninsula) and 10°N–20°N, 97°E–105°E (region B, Indo China Peninsula).

[44] In Figure 9a, average PAR and its standard deviation except strong smoke periods (August to November 1997 and March to April 1998) were 7.77 and 0.35 MJ m^{-2} d^{-1}, respectively. This indicates that temporal PAR variations were small except the strong smoke periods. Although T_c has seasonal variations with amplitude of 0.1, most of these variations are cancelled out by the seasonal change in PAR_{TOA} by the change of solar elevation angle. Figure 9a also suggests that there are few year-to-year variations on T_c despite the large rainfall variations that were recorded [*Toma et al.*, 2000]. Thus the impact of cloud cover variations on PAR was not as large and the smoke aerosol impact on PAR was more significant for the PAR variations in region A.

[45] In contrast, large temporal PAR variations (average = 7.57 MJ m^{-2} d^{-1}, standard deviation, 0.79) are found in Figure 9b. In this area, the T_c has large seasonal variations

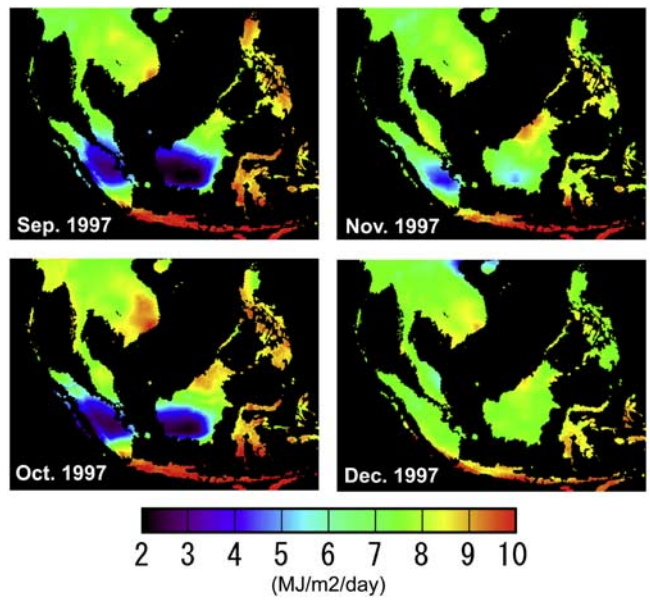

Figure 7. Estimated PAR from September to December 1997 where the large-scale forest fires occurred in Central Kalimantan and Sumatra islands.

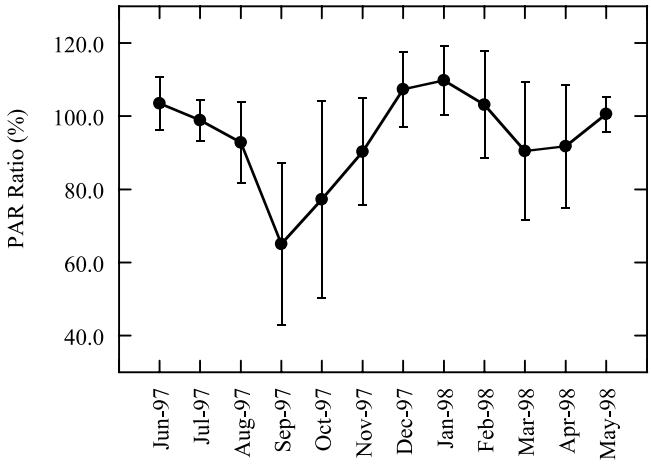

Figure 8. The ratio of PAR in June 1997 to May 1998 to PAR in the corresponding month in 1999 (PAR ratio). The analysis was conducted within 10°N–6.6°S, 94.4°E–119.09°E. The bars show the standard deviation of PAR in this area.

with amplitude of 0.2–0.35, which coincides with wet (May to October) and dry (November to April) seasons and strongly influences in PAR variations. The PAR increases gradually at the end of the dry season and then begins to decrease. Although the phase in PAR and T_c does not match completely due to the seasonal PAR_{TOA} change, the difference between PAR_{TOA} and PAR correlates well with T_c. Thus seasonal variations in PAR were fundamentally regulated by variations in cloud cover on the Indo-China Peninsula.

[46] Year-to-year variations on the region B show that the PAR at the end of the dry season (April and May) remained lower in 1999 than in other years. Maximum PAR in 1999 was 0.8–0.9 MJ m^{-2} d^{-1} lower than in 1997 and 1998 due to a decrease in T_c at the end of dry season. In Figure 9b it is shown that seasonal variations in τ_{550} in 1997, 1998, and 1999 were similar. It peaked with 0.9–1.0 in every March and remained almost constant with 0.4–0.5 in other months. Therefore radiative forcing by smoke aerosol was almost same among these years.

[47] Annual total PAR in two regions discussed above have opposite year-to-year variations. In region A, annual mean PAR in 1997, 1998, and 1999 were 7.39, 7.64, and 7.74 MJ m^{-2} d^{-1}) respectively. The annual mean PAR is small in the El Niño year (1997) rather than the La Niña year (1999), which mainly reflected the extent of smoke impacts. In region B, however, annual mean PAR in 1999 (PAR = 7.31 MJ m^{-2} d^{-1}) was smaller than in 1997 (PAR = 7.61 MJ m^{-2} d^{-1}) and 1998 (PAR = 7.80 MJ m^{-2} d^{-1}), which resulted in the year-to-year variations in cloud cover associated with El Niño and La Niña cycles.

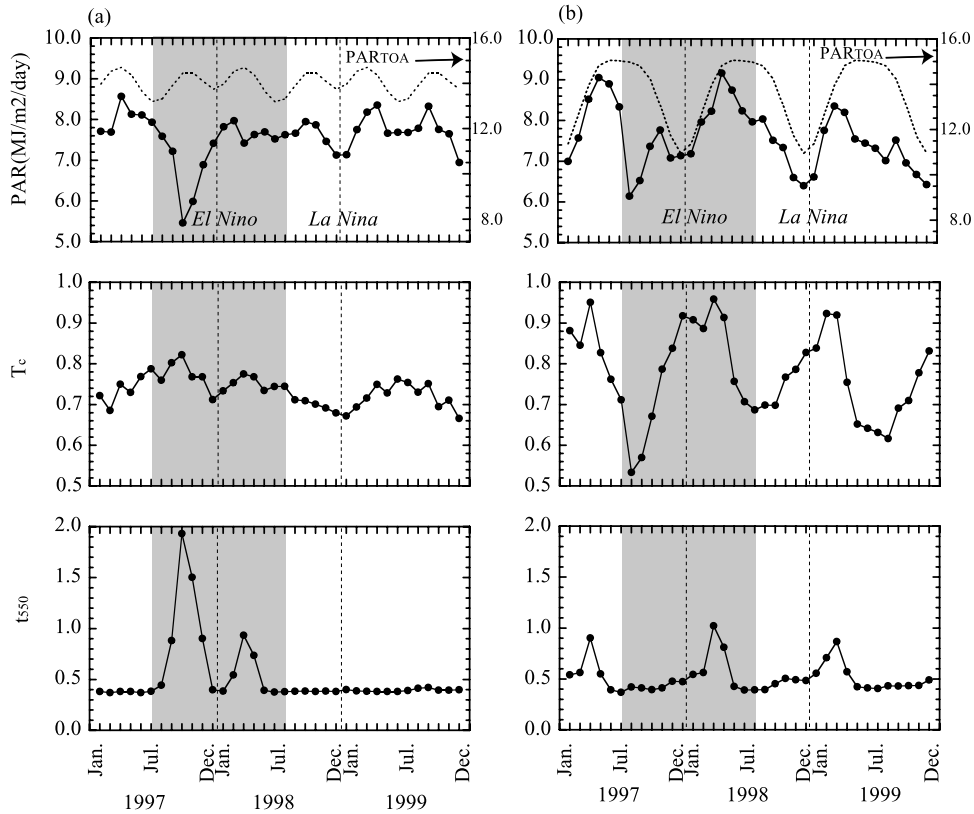

Figure 9. Interannual variation of PAR (MJ m^{-2} d^{-1}), Cloud transmittance (T_c), and aerosol optical thickness at 550 nm. (a) The average of Kalimantan, Sumatra, and southern part of Malay Peninsula (10°N–6.6°S, 94.4°E–119.09°E). (b) The average of Indo-China Peninsula (10°–20°N, 97°E–105°E). The dashed lines in the tope panels indicate the PAR_{TOA}. The El Niño/La Niña period is determined by the Niño 3.4 index.

[48] In Southeast Asia, temporal variations in PAR changed with location. Thus they were not simply correlated with year-to-year cloud cover variations associated with El Niño and La Niña cycles, but reflected on the impact on smoke variations.

5. Conclusions

[49] We developed the simple PAR estimation model to include the smoke effect. The model could estimate monthly PAR with 10% (RMS) accuracy and successfully traced the seasonal and yearly variation in PAR in Southeast Asia. Since we neglected the smoke-cloud interactions and assumed that the smoke was lower than cloud in our model formulation, the model will be limited to these conditions. However, the smoke in the tropics mostly occurs in the dry season. It indicates that the assumption is reasonable in most of the tropics. Also, since we only considered smoke type aerosol, further considerations will be needed to apply the other aerosol cases.

[50] As a result of the analysis, we evaluated the smoke and cloud cover impact on PAR. We found that annual variations in PAR are mostly regulated by smoke variations on the Malay Peninsula, Sumatra, and Kalimantan Islands and cloud cover variations on the Indo-China Peninsula. In Southeast Asia, year-to-year variations of PAR change with location. Thus they did not simply correlate with year-to-year cloud cover variations related to the El Niño and La Niña cycles, but had a more complicated spatial relationship due to the existence of smoke. To establish a precise understanding of the carbon sources and sinks in Southeast Asia, NPP response to PAR should be studied in the future.

[51] **Acknowledgments.** Thanks are extended to the Ozone Processing Team (OPT) for TOMS ozone mapping, NASA/Goddard Space Flight Center for providing the UV reflectivity, the aerosol index, and UV surface reflectivity data, and to Azhar Ishak at the Malaysian Meteorological Service for providing surface pyranometer data in Malaysia.

References

Andreae, M. O., et al. (1988), Biomass-burning emissions and associated haze layers over Amazonia, *J. Geophys. Res.*, *93*(D2), 1509–1527.

Aoki, K., and Y. Fujiyoshi (2003), Sky radiometer measurements of aerosol optical properties over Sapporo, Japan, *J. Meteorol. Soc. Jpn.*, *81*(3), 493–513.

Baker, K. S., and R. Frouin (1987), The relationship between photosynthetically available radiation and total insolation at the ocean surface under clear skies, *Limnol. Oceanogr.*, *32*(6), 1370–1377.

Chameides, W. L., et al. (1999), Case study of the effects of atmospheric aerosols and regional haze on agriculture: An opportunity to enhance crop yields in China through emission controls?, *Proc. Natl. Acad. Sci. U. S. A.*, *96*, 13,626–13,633.

Chu, D. A., Y. K. Kaufman, G. Zibordi, J. D. Chern, J. Mao, C. Li, and B. N. Holben (2003), Global monitoring of air pollution over land from the Earth Obserbing System-Terra Moderate Resolution Imaging Spectrometer (MODIS), *J. Geophys. Res.*, *108*(D21), 4661, doi:10.1029/2002JD003179.

Cohan, D. S., J. Xu, R. Greenwald, M. H. Bergin, and W. L. Chameides (2002), Impact of atmospheric aerosol light scattering and absorption on terrestrial net primary production, *Global Biogeochem. Cycles*, *16*(4), 1090, doi:10.1029/2001GB001441.

Davies, S. J., and L. Unam (1999), Smoke-haze from the 1997 Indonesian forest fires: Effects on pollution levels, local climate, atmospheric CO_2 concentration, and tree photosynthesis, *For. Ecol. Manage.*, *124*, 137–144.

Dye, D. G., and R. Shibasaki (1995), Intercomparison of global PAR data sets, *Geophys. Res. Lett.*, *22*(15), 2013–2016.

Eck, T. F., and D. G. Dye (1991), Satellite estimation of incident photosynthetically active radiation using ultraviolet reflectance, *Remote Sens. Environ.*, *38*, 135–146.

Frouin, R., and R. T. Pinker (1995), Estimating photosynthetically active radiation (PAR) at the Earth's surface from satellite observation, *Remote Sens. Environ.*, *51*, 98–107.

Frouin, R., D. W. Lingner, C. Gautier, K. S. Baker, and R. C. Smith (1989), A simple analytical formula to compute clear sky total and photosynthetically available solar irradiance at the ocean surface, *J. Geophys. Res.*, *94*(C7), 9731–9742.

Goldberg, B., and W. H. Klein (1980), A model for determining the spectral quality of daylight on a horizontal surface at any geographical location, *Sol. Energy*, *24*, 351–357.

Gu, J., and E. A. Smith (1997), High-resolution estimates of total solar and PAR surface fluxes over large-scale BOREAS study area from GOES measurements, *J. Geophys. Res.*, *102*(D24), 29,685–29,705.

Gu, L., J. D. Fuentes, M. Garstang, J. T. da Sliva, R. Heitz, J. Sigler, and H. Shugart (2001), Cloud modulation of surface solar irradiance at a pasture site in southern Brazil, *Agric. For. Meteorol.*, *106*, 117–129.

Gu, L., D. Baldocchi, S. B. Verma, T. A. Black, T. Vesala, E. M. Falge, and P. R. Dowty (2002), Advantages of diffuse radiation for terrestrial ecosystem productivity, *J. Geophys. Res.*, *107*(D6), doi:10.1029/2001JD001242.

Gu, L., D. G. Baldocchi, S. C. Wofsy, J. W. Munger, J. J. Michalsky, S. P. Urbansky, and T. A. Boden (2003), Response of a deciduous forest to the Mount Pinatubo eruption: Enhanced photosynthesis, *Science*, *299*(28), 2035–2038.

Gurney, K. R., et al. (2002), Towards robust regional estimates of CO_2 sources and sinks using atmospheric transport models, *Nature*, *415*, 626–629.

Herman, J. R., and E. A. Celarier (1997), Earth surface reflectivity climatology at 340–380 nm from TOMS data, *J. Geophys. Res.*, *102*(D23), 28,003–28,011.

Herman, J. R., P. K. Bhartia, O. Torres, C. Hsu, C. Seftor, and E. Celarier (1997), Global distribution of UV-absorbing aerosols from Nimbus 7/TOMS data, *J. Geophys. Res.*, *102*(D14), 16,911–16,922.

Hsu, N. C., J. R. Herman, O. Torres, B. N. Holben, D. Tanre, T. F. Eck, A. Smirnov, B. Chatenet, and F. Lavenu (1999), Comparisons of TOMS aerosol index with Sun-photometer aerosol optical thickness: Results and applications, *J. Geophys. Res.*, *104*(D6), 6269–6279.

Hsu, N. C., J. R. Herman, and S. C. Tsay (2003), Radiative impacts from biomass burning in the presence of clouds during boreal spring in southeast Asia, *Geophys. Res. Lett.*, *30*(5), 1224, doi:10.1029/2002GL016485.

Ishida, A., T. Toma, and Marjenah (2000), Leaf gas exchange and canopy structure in wet and drought years, in *Macaranga Conifera: A Tropical Pioneer Tree*, edited by E. Guhardja et al., pp. 29–45, Springer-Verlag, New York.

Kalnay, E., et al. (1996), The NCEP/NCAR 40-year reanalysis project, *Bull. Am. Meteorol. Soc.*, *77*(3), 437–471.

Koe, L. C. C., A. F. Arellano Jr., and J. L. McGregore (2001), Investigating the haze transport from 1997 biomass burning in Southeast Asia: Its impact upon Singapore, *Atmos. Environ.*, *35*, 2723–2734.

Krotkov, N. A., J. R. Herman, P. K. Bhartia, V. Fioletov, and Z. Ahmad (2001), Satellite estimation of spectral surface UV irradiance: 2. Effect of homogeneous clouds and snow, *J. Geophys. Res.*, *106*(D11), 11,743–11,759.

McPeters, R. D., et al. (1998), Earth Probe Total Ozone Mapping Spectrometer (TOMS) data products user's guide, *NASA Tech. Publ., 1998-206895*, 1–64.

Mori, T. (2000), Effect of droughts and forest fires on Depterocarp forest in East Kalimantan, in *Rainforest Ecosystems of East Kalimantan*, edited by E. Guhardja et al., pp. 29–45, Springer-Verlag, New York.

Nakajima, T., A. Higurashi, N. Takeuchi, and J. R. Herman (1999), Satellite and ground-based study of optical properties of 1997 Indonesian forest fire aerosols, *Geophys. Res. Lett.*, *26*(16), 2421–2424.

Nemani, R. R., C. D. Keeling, H. Hashimoto, W. M. Jolly, S. C. Piper, C. J. Tucker, R. B. Myneni, and S. W. Running (2003), Climate-driven increases in global terrestrial net primary production from 1982 to 1999, *Science*, *300*, 1560–1563.

NOAA National Climatic Data Center (2002), Global daily summary of day, http://lwf.ncdc.noaa.gov/.

Page, S. E., F. Siegert, J. O. Rieley, H. V. Boehm, A. Jaya, and S. Limin (2002), The amount of carbon released from peat and forest fires in Indonesia during 1997, *Nature*, *420*, 61–65.

Pinker, R. T., and I. Laszlo (1992), Modeling surface solar irradiance for satellite applications on a global scale, *J. Appl. Meteorol.*, *31*, 194–211.

Reichenau, T. G., and G. Esser (2003), Is interannual fluctuation of atmospheric CO_2 dominated by combined effects of ENSO and volcanic aerosols?, *Global Biogeochem. Cycles*, *17*(4), 1094, doi:10.1029/2002GB002025.

Running, S. W., R. Nemani, J. M. Glassy, and P. E. Thornton (1999), MODIS daily photosynthesis (PSN) and annual net primary production

(NPP) product (MOD17) algorithm theoretical basis document (online), *SCF At-Launch Algorithm ATBD Doc.*, 1–59, Univ. of Mont., Missoula.

Schafer, J. S., B. N. Holben, T. F. Eck, M. A. Yamasoe, and P. Artaxo (2002), Atmospheric effects on insolation in the Brazilian Amazon: Observed modification of solar radiation by clouds and smoke and derived single scattering albedo of fire aerosols, *J. Geophys. Res.*, *107*(D20), 8074, doi:10.1029/2001JD000428.

Tang, Y., N. Kachi, A. Furukawa, and A. Muhamad (1996), Light reduction by regional haze and its effect on simulated leaf photosynthesis in a tropical forest in Malaysia, *For. Ecol. Manage.*, *89*, 205–211.

Toma, T., Marjenah, and Hastaniah (2000), Climate in Bukit Soeharto, East Kalimantan, in *Rainforest Ecosystems of East Kalimantan*, edited by E. Guhardja et al., pp. 13–25, Springer-Verlag, New York.

Torres, O., P. K. Bhartia, J. R. Herman, Z. Ahmad, and J. Gleason (1998), Derivation of aerosol properties from satellite measurements of backscattered ultraviolet radiation: Theoretical basis, *J. Geophys. Res.*, *103*(D14), 17,099–17,110.

Torres, O., P. K. Bhartia, J. R. Herman, A. Synyuk, P. Ginoux, and B. Holben (2002), A long-term record of aerosol optical depth from TOMS observations and comparison to AERONET measurements, *J. Atmos. Sci.*, *59*, 398–413.

Vermote, E. F., D. Tanré, J. L. Deuzé, M. Herman, and J. J. Morcrette (1997), Second simulation of satellite signal in the solar spectrum, 6S: An overview, *IEEE Trans. Geosci. Remote Sens.*, *35*(3), 675–686.

von Hoyningen-Huene, W., T. Schmidt, S. Schienbein, C. A. Kee, and L. J. Tick (1999), Climate-relevant aerosol parameters of South-East-Asian forest fire haze, *Atmos. Environ.*, *33*, 3183–3190.

Wooster, M. J., and N. Strub (2002), Study of the 1997 Borneo fires: Quantitative analysis using global area coverage (GAC) satellite data, *Global Biogeochem. Cycles*, *16*(1), 1009, doi:10.1029/2000GB001357.

M. Aoki, Faculty of Agriculture, Tokyo University of Agriculture and Technology, Saiwaicho 3-5-8, Fuchu, Tokyo 183-8509, Japan.

S. Boonyawat, Faculty of Forestry, Kasetsart University, 50 Phahon Yothin Road, Cha-tuchak, Bangkok 10900, Thailand.

A. Hoyano and H. Kobayashi (corresponding author), Interdisciplinary Graduate School of Science and Technology, Tokyo Institute of Technology, Nagatsuta 4259-G5-407, Midori-ku, Yokohama, Kanagawa 226-8502, Japan. (koba_hidekin@hotmail.com)

D. Komori, United Graduate School of Agricultural Science, Tokyo University of Agriculture and Technology, Saiwaicho 3-5-8, Fuchu, Tokyo 183-8509, Japan.

T. Matsunaga, Social and Environmental Division, National Institute for Environmental Studies, Onogawa 16-2, Tsukuba, Ibaraki 305-8506, Japan.